THE JOURNAL OF PHYSICAL CHEMISTRY B

Article

pubs.acs.org/JPCB

Protein Dynamics of Isolated Chains of Recombinant Human Hemoglobin Elucidated by Time-Resolved Resonance Raman Spectroscopy

Kenta Yamada, Haruto Ishikawa, and Yasuhisa Mizutani*

Department of Chemistry, Graduate School of Science, Osaka University, 1-1 Machikaneyama, Toyonaka, Osaka 560-0043, Japan

Supporting Information

ABSTRACT: Protein dynamics of isolated chains of recombinant human adult hemoglobin (rHb) following ligand photolysis were studied by time-resolved resonance Raman spectroscopy. In the time-resolved spectra, we observed frequency shifts of the iron−histidine stretching [ν(Fe-His)] and γ_7 bands and an intensity change of the ν_8 band for both the isolated α- and β-chains, showing that a primary metastable form was present in the initial tens of nanoseconds following the photolysis. Similar spectral changes were reported for human adult hemoglobin and rHb. Common spectral changes between isolated chains and hemoglobin indicated that structural changes reflected by the spectral changes were characteristic of the hemoglobin subunits. The heme modes suggested that the primary metastable form had a more disordered orientation of propionates and a less strained environment than the deoxy form. The spectral changes of the isolated α-chain were faster than those of the β-chain. In spite of the fact that the isolated β-chain formed a tetramer in a similar fashion to rHb, the spectral changes were much slower than those of rHb. The present study shows that intersubunit interactions affected the rates of the structural changes of the heme pocket. Characteristics of the tertiary structure dynamics of hemoglobin are discussed.

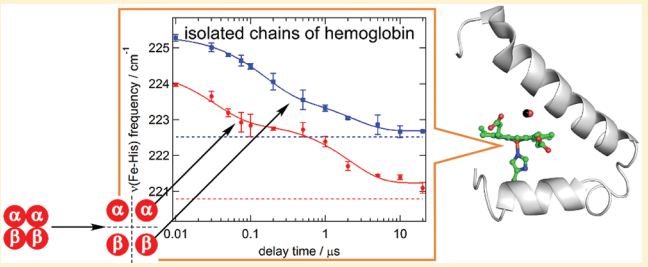

Allostery is a key concept for understanding protein function and regulation.[1] In numerous biological processes, protein structural changes accompanying a reaction at a specific site must undergo global structural changes to perform a biological function. The molecular mechanism of cooperativity in oxygen binding of hemoglobin (Hb) is a classical problem in this regard. Human adult hemoglobin A (HbA) has a tetrameric structure, consisting of two α- and β-subunits. HbA exhibits positive cooperativity in oxygen binding, which is explained in terms of a reversible transition between the two quaternary states upon partial ligation of the four hemes.[2−4] X-ray crystallographic studies[5] have demonstrated the presence of two distinct quaternary structures that correspond to the low-affinity (T or tense) and high-affinity (R or relaxed) states. The completely unligated (deoxy) structure typically adopts the T state, while the fully ligated form adopts the R state.

In HbA, the heme is an iron−protoporphyrin IX, in which the Fe^{2+} ion is bound to the proximal histidine (His) as the only covalent link to the protein. The heme iron binds diatomic molecules, such as O_2, CO, and NO, at the opposite side of the proximal His. Although the binding of small ligands to the hemes in HbA is a highly localized perturbation, this localized perturbation initiates a sequence of propagating structural events that culminates in a change of quaternary structure, proceeding from the T state to the R state. Thus, the protein dynamics inducing the change of quaternary structure must be elucidated to fully understand the allosteric mechanism of Hb.

Time-resolved resonance Raman (RR) spectroscopy provides information on the dynamics of the tertiary and quaternary structures of heme proteins. Along with the studies of Gibson,[6] ligand photolysis techniques have been applied to numerous time-resolved RR studies of HbA.[7−12] In this study, we investigated protein dynamics of isolated chains upon photolysis of carbon monoxide (CO). Isolated chains of HbA remain in oligomeric form but exhibit no cooperativity in oxygen binding and have properties similar to those of myoglobin (Mb). To elucidate what structural dynamics are associated with cooperativity, it is important to compare the dynamics between HbA and the isolated chains. It remains unclear why HbA needs two kinds of chains to function, although some Hbs are homo-oligomers.[13−16] To clarify the reason for this, it is necessary to compare the dynamics between the isolated α- and β-chains because of their different structures[17] and ligand binding properties.[18] Accordingly, knowledge of the properties of each individual subunit in the isolated state is necessary to understand the molecular mechanism of Hb cooperativity.

In this study, we studied protein dynamics of recombinant human Hb (rHb) and its isolated chains using time-resolved RR spectroscopy. The both isolated chains exhibited spectral changes similar to those of rHb upon the CO photolysis, but

Received: November 28, 2011
Revised: January 16, 2012
Published: January 20, 2012

dx.doi.org/10.1021/jp2114303 | J. Phys. Chem. B 2012, 116, 1992−1998

rates of the spectral changes were distinctly different between the isolated chains and rHb. It was also found that the isolated α-chain showed faster spectral changes than the isolated β-chain upon the ligand photolysis. Structural changes of Hb going from the ligated to the deoxy forms are discussed based on comparison of the spectral changes.

EXPERIMENTAL SECTION

Protein Expression and Purification. Recombinant human Hb was expressed in *E. coli* SGE1661 and purified according to previously described procedures.[19,20] The pSGE1702 expression vector contains one copy each of α-globin and β-globin genes, in which the valine residues at the N-terminal are replaced by methionine. Since the oxygen affinity of the α(V1M)/β(V1M) mutant Hb is virtually identical to that of native HbA, the double mutant Hb will be referred to as wild-type rHb.[19,20]

Cells were grown at 37 °C in LB + tetracycline media to OD_{600} of 0.8. After OD_{600} reached 0.8, the rHb protein was then induced with IPTG at a final concentration of 0.2 mM and growth continued at 28 °C for 6−10 h. Excess heme was added throughout the expression phase for a total of 40 mg/L. *E. coli* cells were harvested by centrifugation and then stored at −80 °C. Cells were lysed by sonication and rHb was purified using the chelating Sepharose (GE Healthcare, Chelating Sepharose Fast Flow) column preloaded with Zn^{2+}.[19]

To obtain the isolated α- and β-chains, purified rHb solution was mixed with *p*-mercuribenzoate (PMB) solution at a ratio of 10 mg PMB to 220 mg rHb and left overnight at 4 °C.[19,21] The PMB-bound protein solution was buffer-exchanged against 10 mM sodium phosphate, pH 8.0. Chromatography was performed on a DEAE-cellulose (Whatman, DE52) column equilibrated with 10 mM sodium phosphate buffer, pH 8.0. Isolated α-chain modified by PMB (α-PMB) passed through the column without binding and was collected, and then the residual rHb was washed out with 20 mM sodium phosphate buffer, pH 7.5. Isolated β-chain modified by PMB (β-PMB) was eluted with 100 mM sodium phosphate buffer, pH 7.0. To remove bound PMB from the isolated α- and β-chains, dithiothreitol (DTT) was added to a concentration of 20 mM.[19,21] The isolated chains were separated from the DTT−PMB complex by passage through a Sephadex G-25 column (GE Healthcare, PD-10). The extent of removal was examined by PMB titration.[22] Purity of the isolated chains was confirmed by SDS-PAGE.

Time-Resolved Resonance Raman Measurements. Nanosecond time-resolved RR measurements were performed with two nanosecond pulse lasers operating at 1 kHz. Probe pulses at 436 nm were second harmonics of the output of an Nd:YLF-pumped Ti:sapphire laser (Photonics Industries, TU-L). The probe power was set as low as possible (0.5 μJ/pulse) in order to avoid ligand photolysis by the probe pulse. The pump pulses at 532 nm were generated with a diode-pumped Nd:YAG laser (Megaopto, LR-SHG), the power of which was adjusted to 185 μJ/pulse. These pump and probe beams were directed collinearly using a dichroic mirror and focused onto the sample cell with spherical and cylindrical lenses. Pulse widths of the pump and probe pulses were 20 and 25 ns, respectively. The timing between the pump and probe pulses was adjusted with a computer-controlled pulse generator (Stanford Research Systems, DG 535) via a GPIB interface. Jitters in the delay time were within ±5 ns. Time-resolved RR data acquisition was carried out as described previously.[23] The time delay of the probe pulse with respect to the pump pulse was determined by detecting the two pulses with a photodiode (Electro-Optics Technology, ET-2000) just before the sample point and monitoring with an oscilloscope (Iwatsu, Waverunner DS-4262).

The sample solution was contained in an airtight 10 mm diameter NMR tube and spun with a spinning cell device designed to minimize off-center deviation during rotation. Raman scattered light was detected with a liquid nitrogen-cooled charge-coupled device camera (Roper Scientific, Spec-10:400B/LN) attached to a custom-made prism prefilter (Bunko Keiki) equipped with a single spectrograph (HORIBA, iHR550). The spectra were calibrated using the standard Raman spectra of cyclohexane and carbon tetrachloride.

RESULTS

Figures 1A and 1B show nanosecond time-resolved RR spectra of the isolated α- and β-chains of rHb, respectively, following the CO photolysis in the 1000−1700 cm^{-1} region at various delay times. The fraction of photolyzed species was estimated to be 85 ± 2% based on the intensity loss of the Raman bands of the CO-bound species. In these spectra, the contribution from unreacted species has been subtracted. The band intensities in the spectra at 20 μs are weaker than those in the other time-resolved spectra. This is due to population changes in the photolyzed species resulting from geminate ligand recombination. The 1000−1700 cm^{-1} region of the spectrum for a 30 ns delay contains only the bands arising from the in-plane vibrations of the heme at 1355 (ν_4), 1470 (ν_3), 1567 (ν_2), and 1622 cm^{-1} (ν_{10}) for the α-chain and at 1354 (ν_4), 1470 (ν_3), 1567 (ν_2), and 1623 cm^{-1} (ν_{10}) for the β-chain. The mode assignments made by Abe were adopted.[24] Upon the CO dissociation, the ν_2, ν_3, and ν_{10} bands exhibited a downshift from those of the CO-bound form, indicating that the core size of the heme expands.[25−28] Slight upshifts were observed for the Raman bands of both the isolated α- and β-chains as the delay time increased. Such frequency shifts of the bands have been reported for HbA.[12,29,30] With the exception of slight upshifts, the spectra at 30 ns resemble the spectra of the deoxy form, indicating that the core size expansion of the heme was accomplished within 30 ns after the ligand photolysis.

Figures 2A and 2B show nanosecond time-resolved RR spectra of the isolated α- and β- chains of rHb, respectively, following the CO dissociation in the 180−850 cm^{-1} region. The bands at 224 (225), 303 (303), 344 (346), 365 (365), 403 (409), 672 (673), 755 (756), and 789 (790) cm^{-1} in the 30 ns delay spectrum of the α (β)-chain are assigned to vibrations of the heme. The RR band at 224 (225) cm^{-1} arises from the stretching mode of the covalent bond between the heme iron and the N_ε of the proximal His, ν(Fe-His).[31] The band at 303 (303) cm^{-1} is an out-of-plane mode (γ_7; methine wagging).[32] The band at 344 (346) cm^{-1} was assigned to ν_8, a metal−pyrrole stretch and substituents bend. The bands at 365 (365) and 403 (409) cm^{-1} are substituent modes, $\delta(C_\beta C_c C_d)$, involving deformation of the propionate methylene groups, and $\delta(C_\beta C_a C_b)$, involving deformation of the vinyl groups, respectively. The $\delta(C_\beta C_a C_b)$ frequency was different between the isolated α- and β-chains at 30 ns. This suggests difference in environments around the vinyl groups between the isolated α- and β-chains. A similar frequency difference was observed for the deoxy forms in Figure 2 and in the reported spectra.[12,33] The band at 672 (673) cm^{-1} is assigned to the ν_7 band due to a breathing-like mode of the porphyrin inner ring.

dx.doi.org/10.1021/jp2114303 | J. Phys. Chem. B 2012, 116, 1992−1998

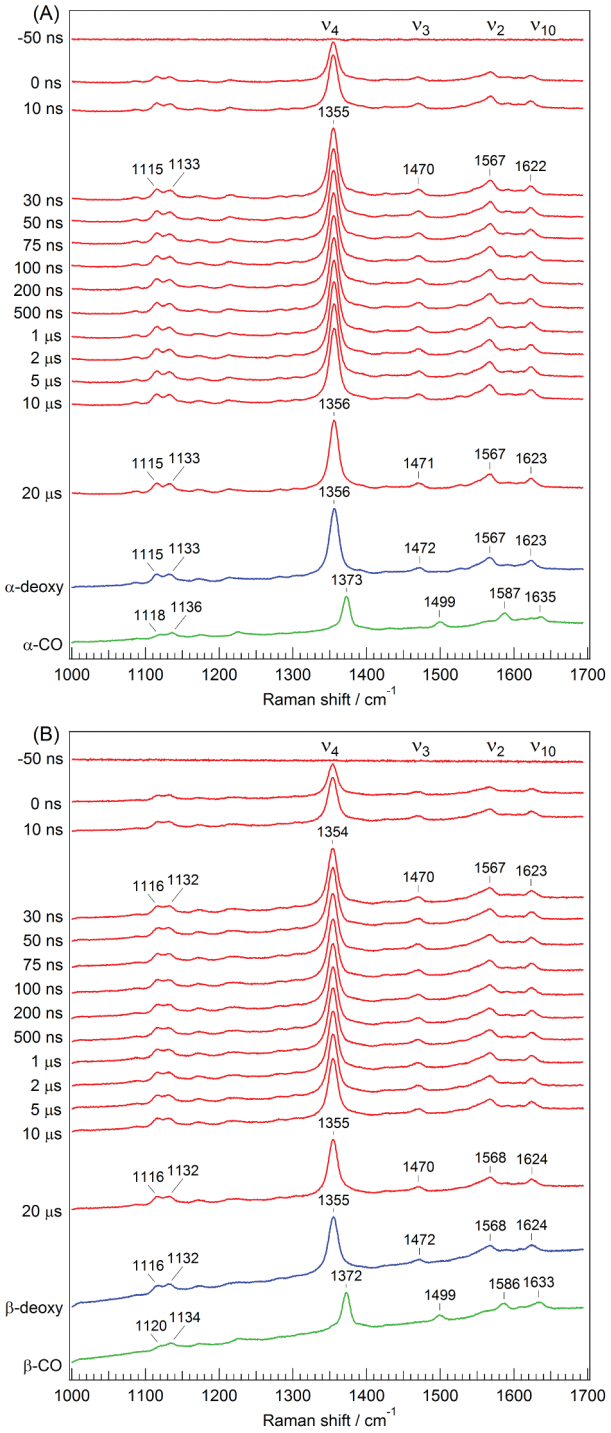

Figure 1. Time-resolved RR spectra in the 1000−1700 cm^{-1} region at the indicated delay times for carbonmonoxy isolated α- (A) and β-chains (B) following the CO photolysis. Spectra of the equilibrium states of the deoxy and CO-bound forms are depicted at the bottom for comparison. Time-resolved difference spectra were generated by subtracting the probe-only spectrum from the pump−probe spectrum at each delay time. The accumulation time for obtaining each spectrum was 18 min.

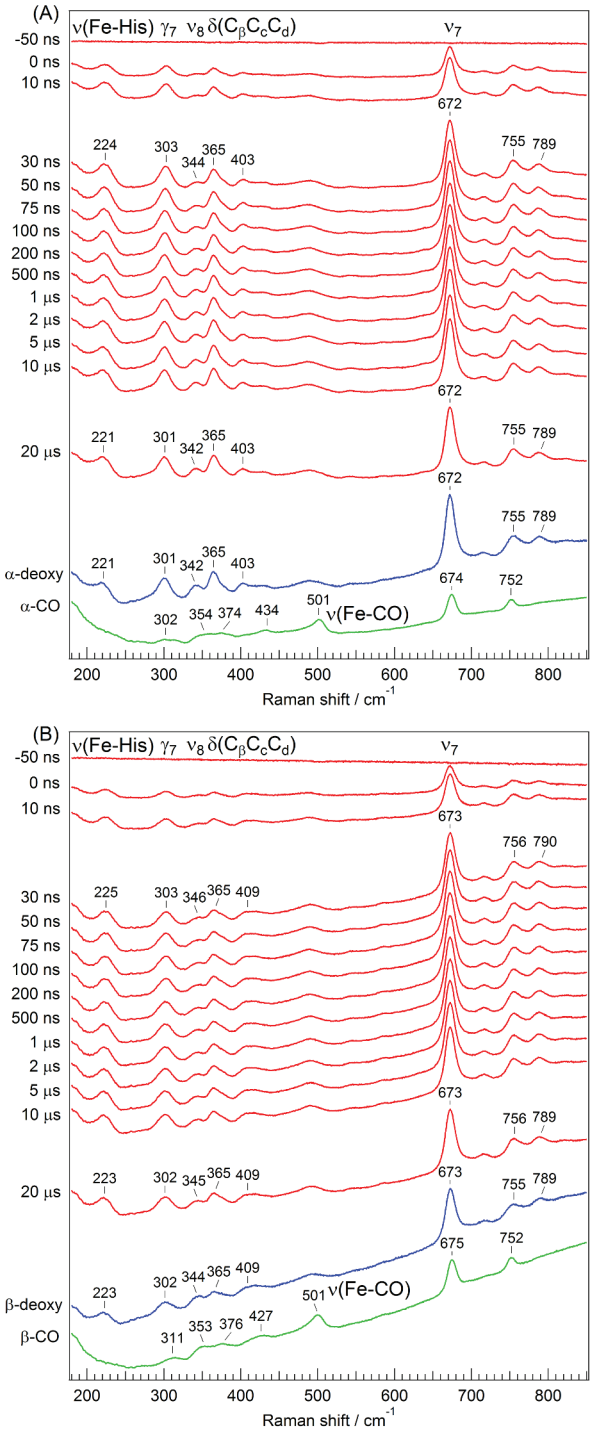

Figure 2. Time-resolved RR spectra in the 180−850 cm^{-1} region at the indicated delay times for carbonmonoxy isolated α- (A) and β-chains (B) following the CO photolysis. Spectra of the equilibrium states of the deoxy and CO-bound forms are depicted at the bottom for comparison. Time-resolved difference spectra were generated by subtracting the probe-only spectrum from the pump−probe spectra at each delay time. The accumulation time for obtaining each spectrum was 56 min, except for the spectrum of the deoxy form. The accumulation time for the deoxy form was 30 min.

The time-resolved RR spectra at 30 ns differed from the spectra of the deoxy form for both the isolated α- and β-chains. The frequencies of the ν(Fe-His) and γ_7 bands in the 30 ns time-resolved RR spectra were higher than those in the spectra of the deoxy form. The ν_8 bands in the 30 ns time-resolved RR spectra were less prominent than those in the spectra of the deoxy form but became more prominent with increasing delay

dx.doi.org/10.1021/jp2114303 | J. Phys. Chem. B 2012, 116, 1992−1998

time. These results indicated that the heme structure at 30 ns after the CO dissociation is different from that of the deoxy structure. Similar spectral differences between the dissociated and the deoxy forms have been reported for HbA.[12,29,30]

Figure 3 shows nanosecond time-resolved RR spectra of rHb following the CO dissociation in the 180−850 cm^{-1} region.

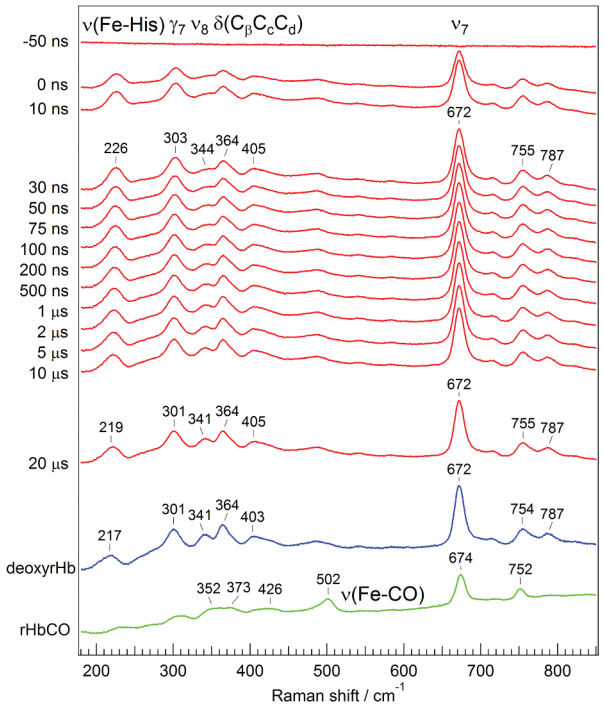

Figure 3. Time-resolved RR spectra in the 180−850 cm^{-1} region at the indicated delay times for carbonmonoxy rHb following the CO photolysis. Spectra of the equilibrium states of the deoxy and CO-bound forms are depicted at the bottom for comparison. Time-resolved difference spectra were generated by subtracting the probe-only spectrum from the pump−probe spectrum at each delay time. The accumulation time for obtaining each spectrum was 56 min, except for the spectrum of the deoxy form. The accumulation time for the deoxy form was 30 min.

The spectra of rHb exhibited a frequency shift of the ν(Fe-His) and γ_7 bands and an increase in the intensity of the ν_8 bands as the delay time increased. Similar to the isolated chains, the upshifts of the ν_2, ν_3, and ν_4 bands were observed in the high-frequency region as the delay time increased (see Figure S1 in the Supporting Information).

Figure 4 compares the temporal evolution of the frequencies of the ν(Fe-His) (A) and γ_7 (B) and intensity of the ν_8 band (C) of rHb and its isolated α- and β-chains following the CO dissociation. The intensity of the ν_8 band was shown in relative value to the intensity of the ν_7 band. The temporal changes of the γ_7 and ν_8 bands were fitted using a single-exponential function for both rHb and its isolated chains. The frequency shift of the ν(Fe-His) band of the isolated chains and rHb were fitted using double- and triple-exponential functions, respectively. The third component of rHb was necessary to express the shift due to the quaternary change. The time constants of the evolutions are summarized in Table 1. The both isolated chains showed slower time evolution than rHb for the all bands analyzed. This indicates that the $\alpha_2\beta_2$ formation affects the structural dynamics of the heme and the heme pocket. The time evolution of the α-chain was faster than that of the β-chain.

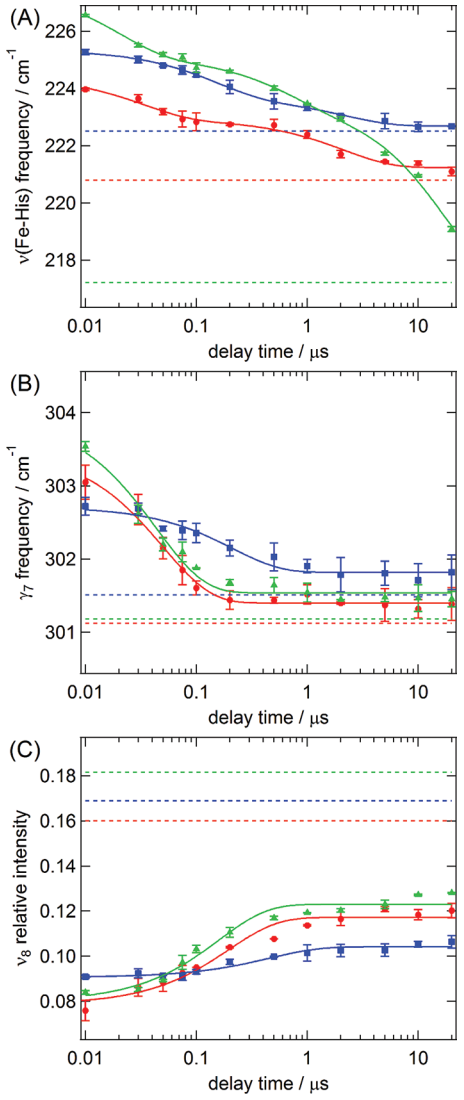

Figure 4. Logarithmic time plots of frequencies of ν(Fe-His) (A) and γ_7 (B) bands and of relative intensity of ν_8 band (C). The solid triangles, circles, and squares represent the frequencies (A, B) and relative intensities (C) of RR bands of rHb and isolated α- and β-chains, respectively. The intensity of the ν_8 band was shown in relative value to the intensity of the ν_7 band. The solid lines indicate the best fit obtained using an exponential function or a sum of exponential functions. The red, blue, and green broken lines show the values of the deoxy forms of the isolated α- and β-chains and rHb, respectively.

The faster spectral changes of the α-chain than those of the β-chain were also observed in the picosecond region.[12] Frequencies of the ν(Fe-His) and γ_7 bands almost approached those of the deoxy form at 20 μs (the longest delay time). In contrast, for the relative intensity of the ν_8 band, there are prominent differences between values at 20 μs and of the deoxy form. The recombination affects the Raman intensities of each band in the observed spectra. But the relative intensities of the deoxy heme were same between the dissociated and deoxy forms if the heme structure of the dissociated form was exactly the same as that of the deoxy form. The present data showed that the relative intensity of the ν_8 band to the ν_7 band is different between the dissociated and deoxy forms. This suggests that the heme structure of the dissociated form at 20 μs is different from that of the deoxy form; namely, structural relaxation is incomplete at 20 μs.

dx.doi.org/10.1021/jp2114303 | J. Phys. Chem. B 2012, 116, 1992−1998

Table 1. Time Constants of Temporal Evolution of Raman Bands of rHb and Its Isolated Chains[a]

		τ_1/ns	τ_2/μs	τ_3/μs
ν(Fe-His)	α-chain	32.8 ± 12.4	2.12 ± 0.56	
	β-chain	146 ± 15	2.19 ± 0.40	
	rHb	20.0 ± 7.1	0.631 ± 0.243	17.3 ± 1.3
γ_7	α-chain	49.9 ± 4.5		
	β-chain	210 ± 50		
	rHb	43.4 ± 5.2		
ν_8	α-chain	197 ± 45		
	β-chain	458 ± 128		
	rHb	159 ± 32		

[a]The temporal evolution is fitted to an exponential function or a sum of exponential functions. The uncertainties shown are 90% confidence levels in the curve fitting.

DISCUSSION

For both isolated chains, the spectral changes in the frequency shift of the ν(Fe-His) and γ_7 bands and the increase in the intensity of the ν_8 bands were observed. Previously, for HbA, it was revealed that the protein adopts a metastable structure within a few picoseconds and does not significantly change in the subnanosecond to nanosecond time after the CO dissociation.[12] The metastable structure was characterized by higher frequencies of the ν(Fe-His) and γ_7 modes and by weaker intensity of the ν_8 bands compared to those of the deoxy form. This intermediate undergoes structural changes in the submicrosecond time frame.[34] The present experimental data indicate that the isolated chains have a similar metastable structure and undergo similar structural changes in the heme to those of rHb and HbA, suggesting that the formation of the metastable structure is characteristic of Hb subunits. The experimental data also indicate that structural changes to the heme later than a nanosecond occur at different rates between the isolated α- and β-chains. Their rates are appreciably different from the rHb, suggesting that the structural dynamics of the chains in the isolated forms are different from those in the subunits.

ν(Fe-His) Band. Kitagawa and co-workers[31,35,36] showed that RR spectra of deoxy forms of heme proteins with an axial ligand of His contain a band in the region between 200 and 250 cm^{-1} assignable to the ν(Fe-His) mode. The intensity and frequency of this band depend strongly on the tertiary and quaternary structures of the respective heme protein.[35,37] The ν(Fe-His) bond in Hb is the sole covalent linkage between the heme and the protein. Consequently, this mode is a good indicator of heme protein tertiary and quaternary structures. The ν(Fe-His) band was observed only in the unligated ferrous form of heme proteins. This was explained by the proposal that the origin of the intensity of the ν(Fe-His) mode results from orbital overlap between the σ*-orbital of the Fe-His bond and the π*-orbital of the porphyrin ring, which is small in the planar structure but becomes large in the domed structure.[38]

It is well recognized that the proximal Fe-His linkage in heme proteins plays a pivotal role in communicating protein structural changes to the functional heme group, thus affecting its biological properties.[39] When the deoxy form of Hb changes its quaternary structure from the R to the T state, the ν(Fe-His) band shifts to lower frequencies. In the deoxy form within the quaternary T state, the frequency of the band is 216 cm^{-1}, whereas the R state of the modified deoxy NES-des(Arg141α)-Hb exhibits a Raman band at a frequency of 221 cm^{-1}.[40] Matsukawa et al. observed a definite correlation between the ν(Fe-His) frequency and the first Adair constant K_1, which is related to the Gibbs energy of the first oxygenation step.[41] This finding was explained in terms of Perutz's strain model.[4,5] Hence, the ν(Fe-His) band became a prominent marker band in the investigation of the relationship between structure and function of this class of proteins.

The temporal changes of the ν(Fe-His) band of HbA were studied by time-resolved RR spectroscopy over a wide time range. In the low-frequency region of the RR spectrum, it has been shown that the ν(Fe-His) RR band is absent from the CO-bound form of HbA but appears at a shifted position of 223 cm^{-1} in photolyzed (R state) HbA as measured at 3 ps,[12] later relaxing to the equilibrium (T state) deoxy position of 210−216 cm^{-1} on the 100 ns to microsecond time scale.[10]

The difference in the ν(Fe-His) frequencies of the T and R states of the Hb forms was attributed to a difference in the azimuthal angle.[38] Peterson et al. measured the ν(Fe-His) frequencies of several mutants of sperm whale Mb and observed a correlation between the ν(Fe-His) frequency and heme proximal-His geometry.[42] Changes in the ν(Fe-His) frequency were attributed to changes in the azimuthal angle of the His imidazole ring driven by a change in steric factors. Samuni et al. reported that the ν(Fe-His) frequencies of truncated Hbs were higher than those of Mb.[43] The difference in the frequency was also attributed to the difference in azimuthal angle. Crystallographic structural data of the isolated β chain showed that the azimuthal angle is different between the CO-bound and deoxy form.[44] Thus, it is highly likely that the frequency shift of the ν(Fe-His) mode observed in this study is due to the change in the azimuthal angle in the structural relaxation following the CO dissociation.

γ_7 Band. The heme γ_7 band at ∼300 cm^{-1} has been shown to be sensitive to proximal strain with lower frequencies, which is indicative of increased proximal strain.[45] Thus, it is suggested that the increase of the proximal strain is faster in the isolated β-chain than in the isolated α-chain. This is consistent with the experimental observation that the ν(Fe-His) frequency of the isolated β-chain shifted more slowly than that of the isolated α-chain.

ν_8 Band. The intensity of the ν_8 band changed after the CO dissociation. It has been suggested that the intensity of this band is correlated with disorder in the orientation of the propionate groups.[42] As this disorder increases, the ν_8 band intensity decreases. For example, the ν_8 band of HbA appeared when the heme propionates were motionally restricted in a trehalose glass.[46] X-ray crystallographic data suggest that heme propionate 7 forms a hydrogen bond with Lys61α(E10) in the α-subunits and with Lys66β(E10) in the β-subunits upon formation of the deoxy form, which is not formed in the CO-bound form.[47] The propionate 6 forms hydrogen bonds with His58α(E7) and Lys61α(E10) in the α-subunits of the deoxy form, while they are absent in the CO-bound form. In contrast, neither the change of the propionate nor the intensity of the ν_8 band was observed in Mb upon formation of the deoxy form. Accordingly, the increase in ν_8 band intensity is attributed to the formation of hydrogen bonds that restrict the orientation of the heme propionates. The fact that the rates of the change of the ν_8 band were slower than those of the ν(Fe-His) and γ_7 bands suggests that the formation of the hydrogen bond is slower than the increase of the proximal strain upon the CO dissociation.

Structural Changes of Hb from the Ligated to the Deoxy Forms. Previous time-resolved absorption[48] and RR[8,12,49] spectroscopic studies on HbA have established a series of intermediates following the CO dissociation. In primary intermediate B, the heme structure changes to a metastable form similar to that of the deoxy form, but no detectable difference was found in the globin structure between intermediate B and the CO-bound form. The dissociated CO from the heme has not yet left the heme pocket and docked in the vicinity of the heme.[50,51] Protein relaxation leads to the secondary intermediate, R_{deoxy}. In the transition from B to R_{deoxy}, the distal E helix displaces toward the heme plane, probably driven by motion of the proximal F helix in response to Fe-His bond relaxation.[8,49,52] For the CO photolysis, this displacement occurs in tens of nanoseconds, which coincides with spectral changes of the ν(Fe-His) and γ_7 bands. The structural change seen beyond 10 ps for the heme in HbA does not indicate an intrinsic change in the nature of the heme group but is associated with structural changes of the globin (protein moiety). The frequency shift was not observed for the ν(Fe-Im) band of the model compound without protein matrix, hemin−2-methylimidazole complex,[23] indicating that the structural change seen for HbA is not a characteristic of the heme−histidine (or imidazole) unit and that it is associated with protein relaxation. Therefore, we can speculate that the structural changes of the heme in terms of the proximal strain and the hydrogen bonds of the propionates are associated with the EF helical motion in the B−R_{deoxy} transition.

X-ray crystallographic data showed that the E helix is displaced from the CO-bound form to the deoxy form. Interestingly, the magnitude of the displacement was different between the α- and β-subunits of HbA: the displacement is larger in the β-subunit than in the α-subunit. Since, upon the CO dissociation, a larger displacement should take a longer time, the difference in the displacement of the E-helix can result in differences in the rate of EF helical motion after ligand dissociation. This explains the chain dependence of the protein dynamics. Another possible reason for the chain-dependent rates of the dynamics is the difference in the oligomerization of the isolated chains: the isolated α- and β-chains form dimer/monomer and tetramer, respectively.[53] The larger size of the oligomer in the β-chain and/or a different fashion of intersubunit interaction may reduce the rate of the structural dynamics.

The dissociated CO undergoes geminate recombination at room temperature. A fraction of the docked ligand diffuses into the heme pocket and rebinds. The rates of geminate rebinding for CO reported for the isolated α- and β-chains are 20 and 7.1 μs^{-1},[18] respectively. Rates determined based on Raman intensities of the ν_4 band were consistent with the reported rates (see Figure S2 in the Supporting Information). Interestingly, these rebinding rates and the rates of the B to R_{deoxy} transition observed in the time-resolved RR spectra are of the same order of magnitude. This similarity can be explained as follows. If intermediates B and R_{deoxy} have slow and fast intrinsic rebinding rates, respectively, the apparent geminate rebinding rate is determined by the rate of the transition from B to R_{deoxy}. In R_{deoxy}, the E-helix is displaced toward the heme plane.[54] The displacement reduces the volume accessible for the ligand to diffuse and hence accelerates geminate rebinding in R_{deoxy}. Therefore, it is likely that the structural changes in the B−R_{deoxy} transition are associated with the ligand rebinding process.

The rates of the isolated chains were different from those of rHb. This indicates that the protein dynamics are affected by the formation of the $\alpha_2\beta_2$ tetramer. Differences between the isolated chains and the $\alpha_2\beta_2$ tetramer were also observed in the geminate recombination rates[18] and CD spectra.[17] These results show that the intersubunit interactions induce changes in the tertiary structure of HbA. Matsukawa et al. showed that the strain imposed on the Fe−His bond by the globin was influenced by mutations at the α−β-subunit interface.[41] This and the present studies suggested that interactions at the subunit interface affect the structure and the rates of the structural changes in the heme pocket, respectively. This is consistent with the Perutz model, in which the cooperativity consists of a change in tension at the heme, brought about by the transition between the two alternative quaternary structures.[4,5]

■ CONCLUSIONS

In this study, we closely examined the temporal behavior of time-resolved RR spectra of rHb and its isolated chains. The spectral changes in the frequency shift of the ν(Fe-His) and γ_7 bands and the increase in the intensity of the ν_8 bands were observed commonly in the isolated chains and rHb, suggesting that structural changes reflected by the spectral changes are characteristic of Hb subunits. The rates of the changes were different between the chains. The rates of the changes of the α-chain were faster than those of the β-chain. We discussed characteristics of the protein dynamics of the isolated chains based on comparison of the results with rHb. It was suggested that the primary metastable form of the isolated chains had a more disordered orientation of propionate groups and a less strained environment than the deoxy form. The present study suggested that interactions at the subunit interface affected the rates of the structural changes in the heme pocket.

■ ASSOCIATED CONTENT

Supporting Information

Time-resolved RR spectra of carbonmonoxy rHb following the CO dissociation in the 1000−1700 cm^{-1} region and fractions of the CO-bound form of the isolated α- (A) and β-chains (B) in the range of −0.05 to 5 μs. This material is available free of charge via the Internet at http://pubs.acs.org.

■ AUTHOR INFORMATION

Corresponding Author

*Ph: +81-6-6850-5776; Fax: +81-6-6850-5776; e-mail: mztn@chem.sci.osaka-u.ac.jp.

Notes

The authors declare no competing financial interest.

■ ACKNOWLEDGMENTS

The authors thank Professor John S. Olson and Dr. Eileen Singleton for providing the pSGE1702 plasmid and *E. coli* SGE1661 and instructions on the procedures of protein expression purification. The authors thank Professor Masako Nagai of Hosei University for her valuable advice on the preparation of the isolated chains. This work was supported in part by a Grant-in-Aid for Scientific Research on the Priority Area "Molecular Science for Supra Functional Systems" (Grant No. 19056013) to Y.M. from the Ministry of Education, Science, Sports, and Culture of Japan.

REFERENCES

(1) Monod, J.; Wyman, J.; Changeux, J.-P. *J. Mol. Biol.* **1965**, *12*, 88−118.
(2) Perutz, M. F. *Annu. Rev. Biochem.* **1979**, *48*, 327−386.
(3) Perutz, M. F.; Fermi, G.; Luisi, B.; Shaanan, B.; Liddington, R. C. *Acc. Chem. Res.* **1987**, *20*, 309−321.
(4) Perutz, M. F. *Nature* **1972**, *237*, 495−499.
(5) Perutz, M. F. *Nature* **1970**, *228*, 726−739.
(6) Gibson, Q. H. *Biochem. J.* **1959**, *71*, 293−290.
(7) Franzen, S.; Bohn, B.; Poyart, C.; Martin, J. L. *Biochemistry* **1995**, *34*, 1224−1237.
(8) Jayaraman, V.; Rodgers, K. R.; Mukerji, I.; Spiro, T. G. *Science* **1995**, *269*, 1843−1848.
(9) Rodgers, K. R.; Spiro, T. G. *Science* **1994**, *265*, 1697−1699.
(10) Scott, T. W.; Friedman, J. M. *J. Am. Chem. Soc.* **1984**, *106*, 5677−5687.
(11) Scott, T. W.; Friedman, J. M.; Macdonald, V. W. *J. Am. Chem. Soc.* **1985**, *107*, 3702−3705.
(12) Mizutani, Y.; Nagai, M. *Chem. Phys.* **2012**, in press.
(13) Harutyunyan, E. H.; Safonova, T. N.; Kuranova, I. P.; Popov, A. N.; Teplyakov, A. V.; Obmolova, G. V.; Rusakov, A. A.; Vainshtein, B. K.; Dodson, G. G.; Wilson, J. C.; Perutz, M. F. *J. Mol. Biol.* **1995**, *251*, 104−115.
(14) Kolatkar, P. R.; Ernst, S. R.; Hackert, M. L.; Ogata, C. M.; Hendrickson, W. A.; Merritt, E. A.; Phizackerley, R. P. *Acta Crystallogr., Sect. B: Struct. Sci.* **1992**, *48*, 191−199.
(15) Royer, W. E. Jr. *J. Mol. Biol.* **1994**, *235*, 657−681.
(16) Heaslet, H. A.; Royer, W. E. *Structure* **1999**, *7*, 517−526.
(17) Li, R.; Nagai, Y.; Nagai, M. *J. Inorg. Biochem.* **2000**, *82*, 93−101.
(18) Birukou, I.; Maillett, D. H.; Birukova, A.; Olson, J. S. *Biochemistry* **2011**, *50*, 7361−7374.
(19) Birukou, I.; Schweers, R. L.; Olson, J. S. *J. Biol. Chem.* **2010**, *285*, 8840−8854.
(20) Looker, D.; Mathews, A. J.; Neway, J. O.; Stetler, G. L. *Methods Enzymol.* **1994**, *231*, 364−374.
(21) Bucci, E.; Fronticelli, C. *J. Biol. Chem.* **1965**, *240*, PC551−552.
(22) Boyer, P. D. *J. Am. Chem. Soc.* **1954**, *76*, 4331−4337.
(23) Mizutani, Y.; Kitagawa, T. *J. Phys. Chem. B* **2001**, *105*, 10992−10999.
(24) Abe, M.; Kitagawa, T.; Kyogoku, Y. *J. Chem. Phys.* **1978**, *69*, 4526−4534.
(25) Choi, S.; Spiro, T. G.; Langry, K. C.; Smith, K. M.; Budd, D. L.; La Mar, G. N. *J. Am. Chem. Soc.* **1982**, *104*, 4345−4351.
(26) Oertling, W. A.; Salehi, A.; Chung, Y. C.; Leroi, G. E.; Chang, C. K.; Babcock, G. T. *J. Phys. Chem.* **1987**, *91*, 5887−5898.
(27) Spaulding, L. D.; Chang, C. C.; Yu, N.-T.; Felton, R. H. *J. Am. Chem. Soc.* **1975**, *97*, 2517−2525.
(28) Spiro, T. G.; Stong, J. D.; Stein, P. *J. Am. Chem. Soc.* **1979**, *101*, 2648−2655.
(29) Dasgupta, S.; Spiro, T. G. *Biochemistry* **1986**, *25*, 5941−5948.
(30) Friedman, J. M.; Rousseau, D. L.; Ondrias, M. R.; Stepnoski, R. A. *Science* **1982**, *218*, 1244−1246.
(31) Kitagawa, T.; Nagai, K.; Tsubaki, M. *FEBS Lett.* **1979**, *104*, 376−378.
(32) Hu, S.; Smith, K. M.; Spiro, T. G. *J. Am. Chem. Soc.* **1996**, *118*, 12638−12646.
(33) Podstawka, E.; Mak, P. J.; Kincaid, J. R.; Proniewicz, L. M. *Biopolymers* **2006**, *83*, 455−466.
(34) Murakawa, Y.; Nagai, M.; Mizutani, Y. *J. Am. Chem. Soc.* **2012**, *134*, 1434−1437.
(35) Kitagawa, T. The heme protein structure and the iron histidine stretching mode. In *Biological Application on Raman Spectroscopy*; Spiro, T. G., Ed.; John Wiley and Sons: New York, 1988; Vol. *III*, pp 97−131.
(36) Hori, H.; Kitagawa, T. *J. Am. Chem. Soc.* **1980**, *102*, 3608−3613.
(37) Rousseau, D. L.; Friedman, J. M. Transient and cryogenic studies of photodissociated hemoglobin and myoglobin. In *Biological Application on Raman Spectroscopy*; Spiro, T. G., Ed.; John Wiley and Sons: New York, 1988; Vol. *III*, pp 133−216.
(38) Bangcharoenpaurpong, O.; Schomacker, K. T.; Champion, P. M. *J. Am. Chem. Soc.* **1984**, *106*, 5688−5698.
(39) Gelin, B. R.; Lee, A. W.; Karplus, M. *J. Mol. Biol.* **1983**, *171*, 489−559.
(40) Nagai, K.; Kitagawa, T. *Proc. Natl. Acad. Sci. U. S. A.* **1980**, *77*, 2033−2037.
(41) Matsukawa, S.; Mawatari, K.; Yoneyama, Y.; Kitagawa, T. *J. Am. Chem. Soc.* **1985**, *107*, 1108−1113.
(42) Peterson, E. S.; Friedman, J. M.; Chien, E. Y. T.; Sligar, S. G. *Biochemistry* **1998**, *37*, 12301−12319.
(43) Samuni, U.; Ouellet, Y.; Guertin, M.; Friedman, J. M.; Yeh, S.-R. *J. Am. Chem. Soc.* **2004**, *126*, 2682−2683.
(44) Borgstahl, G. E. O.; Rogers, P. H.; Arnone, A. *J. Mol. Biol.* **1994**, *236*, 817−830.
(45) Podstawka, E.; Rajani, C.; Kincaid, J. R.; Proniewicz, L. M. *Biopolymers* **2000**, *57*, 201−207.
(46) Gottfried, D. S.; Peterson, E. S.; Sheikh, A. G.; Wang, J.; Yang, M.; Friedman, J. M. *J. Phys. Chem.* **1996**, *100*, 12034−12042.
(47) Park, S.-Y.; Yokoyama, T.; Shibayama, N.; Shiro, Y.; Tame, J. R. H. *J. Mol. Biol.* **2006**, *360*, 690−701.
(48) Hofrichter, J.; Sommer, J. H.; Henry, E. R.; Eaton, W. A. *Proc. Natl. Acad. Sci. U. S. A.* **1983**, *80*, 2235−2239.
(49) Balakrishnan, G.; Case, M. A.; Pevsner, A.; Zhao, X.; Tengroth, C.; McLendon, G. L.; Spiro, T. G. *J. Mol. Biol.* **2004**, *340*, 843−856.
(50) Lim, M.; Jackson, T. A.; Anfinrud, P. A. *J. Chem. Phys.* **1995**, *102*, 4355−4366.
(51) Lim, M.; Jackson, T. A.; Anfinrud, P. A. *J. Am. Chem. Soc.* **2004**, *126*, 7946−7957.
(52) Balakrishnan, G.; Tsai, C. H.; Wu, Q.; Case, M. A.; Pevsner, A.; McLendon, G. L.; Ho, C.; Spiro, T. G. *J. Mol. Biol.* **2004**, *340*, 857−868.
(53) Valdes, R.; Ackers, G. K. *J. Biol. Chem.* **1977**, *252*, 88−91.
(54) Jayaraman, V.; Spiro, T. G. *Biospectroscopy* **1996**, *2*, 311−316.